Investigation of a general base mechanism for ester hydrolysis in C–C hydrolase enzymes of the α/β-hydrolase superfamily: a novel mechanism for the serine catalytic triad

Jian-Jun Li and Timothy D. H. Bugg*

Received 27th October 2006, Accepted 27th November 2006
First published as an Advance Article on the web 19th December 2006
DOI: 10.1039/b615605c

Previous mechanistic and crystallographic studies on two C–C hydrolase enzymes, *Escherichia coli* MhpC and *Burkholderia xenovorans* BphD, support a general base mechanism for C–C hydrolytic cleavage, rather than the nucleophilic mechanism expected for a serine hydrolase. The role of the active site serine residue could be to form a hydrogen bond with a *gem*-diolate intermediate, or to protonate such an intermediate. Hydrolase BphD is able to catalyse the hydrolysis of *p*-nitrophenyl benzoate ester substrates, which has enabled an investigation of these mechanisms using a Hammett analysis, and comparative studies upon five serine esterases and lipases from the α/β-hydrolase family. A reaction parameter (ρ) value of +0.98 was measured for BphD-catalysed ester hydrolysis, implying a build-up of negative charge in the transition state, consistent with a general base mechanism. Values of +0.31–0.61 were measured for other serine esterases and lipases, for the same series of esterase substrates. Pre-steady state kinetic studies of ester hydrolysis, using *p*-nitrophenyl acetate as the substrate, revealed a single step kinetic mechanism for BphD-catalysed ester hydrolysis, with no burst kinetics. A general base mechanism for BphD-catalysed ester hydrolysis is proposed, in which Ser-112 stabilises an oxyanion intermediate through hydrogen bonding, and assists the rotation of this oxyanion intermediate *via* proton transfer, a novel reaction mechanism for the serine catalytic triad.

Introduction

The serine catalytic triad, found in the serine proteases and in the α/β-hydrolase family of esterases and lipases, is a paradigm of nucleophilic catalysis in enzymology. Enzymes in the α/β-hydrolase family possess a common structural fold consisting of a β-sheet of 5 or 6 parallel β-strands terminating in loops bearing the active site serine, histidine, and aspartate residues.[1,2] Members of the α/β-hydrolase family have in recent years been found to catalyse a surprising range of non-hydrolytic reactions, for example cyanohydrin formation and haloperoxidase activity, raising the question of whether they follow similar catalytic mechanisms.[3]

Mechanistic studies in our laboratory on C–C hydrolase MhpC (2-hydroxy-6-ketonona-2,4-diene 1,9-dioic acid 5,6-hydrolase) from *Escherichia coli*, an enzyme in the α/β-hydrolase family, have implicated a general base mechanism in this enzyme.[4–9] This enzyme catalyses the hydrolytic C–C cleavage of the *meta*-ring fission product on the phenylpropionic acid catabolic pathway.[4] Related C–C hydrolase BphD is found in the bacterial *meta*-cleavage pathway for degradation of biphenyl in *Burkholderia xenovorans* LB400,[5] and similar enzymes are found in other aromatic degradation pathways. Amino acid sequence alignments reveal that these enzymes are members of the α/β-hydrolase family, containing conserved serine (Ser-110 in MhpC, Ser-112 in BphD), histidine (His-263 in MhpC, His-265 in BphD) and aspartate (Asp-235 in MhpC, Asp-237 in BphD) residues which make up the catalytic triad.[6]

The catalytic mechanism for C–C cleavage, shown in Fig. 1, commences by keto–enol tautomerisation of the substrate, to give a keto-intermediate, implicated by stopped flow kinetic analysis,[7] and deuterium isotope exchange studies.[4] Nucleophilic attack on the C-6 carbonyl is then followed by a stereospecific C–C

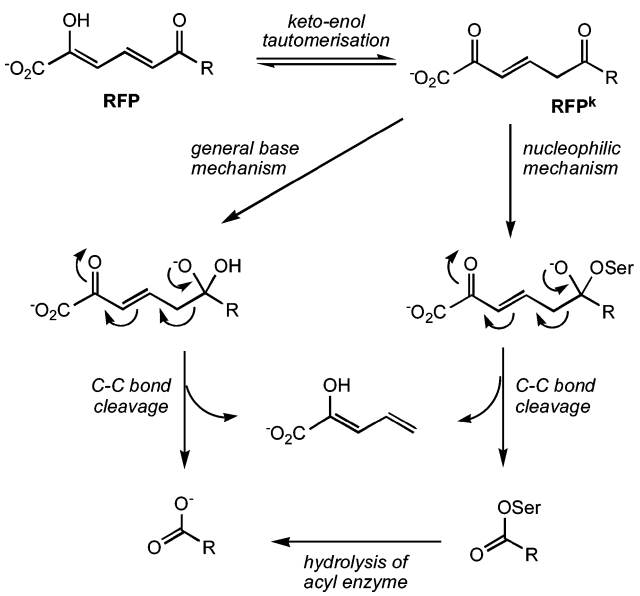

Fig. 1 Reactions catalysed by C–C hydrolases MhpC and BphD, showing keto–enol tautomerisation and general base *vs.* nucleophilic mechanisms.

Department of Chemistry, University of Warwick, Coventry, UK CV4 7AL. E-mail: T.D.Bugg@warwick.ac.uk; Fax: +44 (0)2476-524112; Tel: +44 (0)2476-573018

fragmentation, to give the product 2-hydroxypentadienoic acid (HPD). Deuterium labelling studies on MhpC, and more recently on BphD, have established that the H_{5E} hydrogen is inserted by enzyme-catalysed protonation, thus replacing the succinyl group with hydrogen with overall retention of stereochemistry.[4,8]

If Ser-110 acts as a nucleophile in the mechanism, then an acyl enzyme intermediate would result from C–C cleavage, which would then be hydrolysed to give succinate. Unlike the serine proteases, which accumulate a stoichiometric amount of acyl enzyme intermediate under acidic conditions (pH < 6), MhpC is catalytically active at pH 4.0 (k_{cat} 1.0 s^{-1}), under which conditions the hydrolysis of the putative acyl enzyme intermediate was shown by stopped flow kinetics to be rate-limiting.[7] Attempts to trap the acyl enzyme intermediate under these conditions with ^{14}C-labelled substrate by rapid quench gave stoichiometries of enzyme bound ^{14}C label of < 1%.[9]

Evidence in favour of an alternative mechanism, namely base-catalysed attack of water, has been obtained from $H_2{}^{18}O$ incorporation studies using the natural substrate and a non-cleavable substrate analogue.[9] We have developed a chemical synthesis of aryl-containing substrates for C–C hydrolase BphD, and have measured a Hammett plot for *Burkholderia xenovorans* LB400 BphD, showing a ρ value of −0.70 for C–C cleavage.[10] Furthermore, aldol-type cleavage of a reduced alcohol substrate was observed for BphD, inconsistent with a nucleophilic mechanism.[10] Thus, several independent mechanistic studies indicate a catalytic mechanism involving base-catalysed attack of water, not nucleophilic attack of a serine residue, thereby raising the question of what is the catalytic role of the active site serine residue

The structure of *E. coli* MhpC complexed with the non-cleavable analogue, 2,6-diketonona-1,9-dioic acid (DKNDA), was reported in 2005.[11] The arrangement of active site residues is illustrated in Fig. 2. The analogue is bound in a linear, extended conformation perpendicular to the His-263 and Ser-110 residues, which straddle the bound substrate in an arrangement not seen in the serine proteases. Two possible active site structures could be modelled to the electron density map: one in which Ser-110 is covalently attached to C-6 of the inhibitor *via* a hemi-ketal linkage; and one in which the β-hydroxyl group of Ser-110 is hydrogen-bonded to the C-6 carbonyl group. Kinetic analysis of a S110A site-directed mutant of MhpC revealed that k_{cat} was reduced 10^4-fold in this mutant, which retained a low level of catalytic activity, but K_m was unchanged.[12] Pre-steady state kinetic analysis of this mutant revealed that ketonisation of the dienol substrate occurred at the same rate as with the wild-type enzyme, but that C–C cleavage was

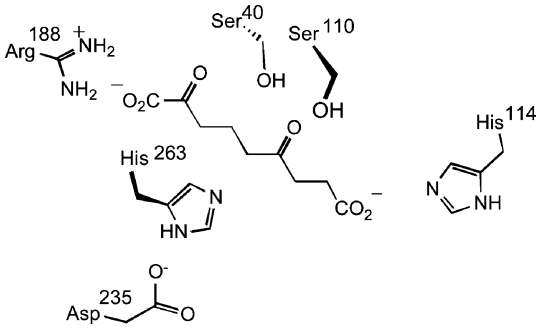

Fig. 2 Active site of *E. coli* MhpC, complexed with DKNDA analogue.

dramatically slowed.[12] Therefore it is apparent that Ser-110 is not involved in initial substrate binding, nor is it involved in keto–enol tautomerisation, but that it has an important role in C–C cleavage.

We have shown previously that *E. coli* MhpC is able to catalyse the hydrolysis of a monoethyl adipate ester substrate.[12] In this paper we show that *B. xenovorans* BphD, whose natural substrate contains an aromatic ring, is able to catalyse the hydrolysis of *p*-nitrophenyl benzoate esters. This observation enables structure–activity studies to study the transition state for ester hydrolysis, and allows a direct comparison with esterases and lipases from the α/β-hydrolase superfamily. Three possible catalytic roles for the active site serine of these enzymes are shown in Fig. 3: A) as a nucleophile; B) as a hydrogen bond donor, forming a hydrogen bond with an oxyanion intermediate; C) as a proton donor, protonating an oxyanion intermediate. Mechanisms A and B would involve build-up of negative charge in the transition state, whereas mechanism C would involve build-up of positive charge in the transition state.

These mechanisms could therefore be analysed using a Hammett plot approach. Furthermore, mechanism A would involve a 2-step reaction with a covalent intermediate, whereas mechanisms B and C both involve 1-step mechanisms. This paper describes kinetic studies using a Hammett plot analysis and pre-steady state kinetic analysis, in order to distinguish these mechanisms.

Results

Synthesis of *p*-nitrophenyl *p*-substituted benzoate substrates

A series of *p*-nitrophenyl *p*-substituted benzoates **1–8** was synthesized, following published procedures (Scheme 1) in 70–80% yields.[13,14]

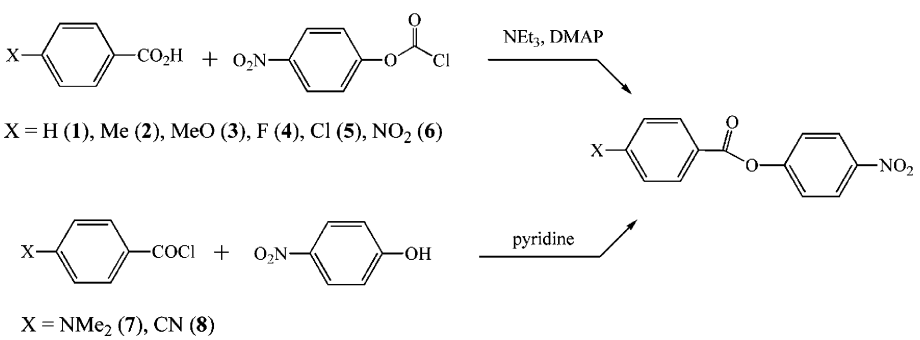

Scheme 1 Preparation of *p*-substituted benzoate substrates.

 This journal is © The Royal Society of Chemistry 2007

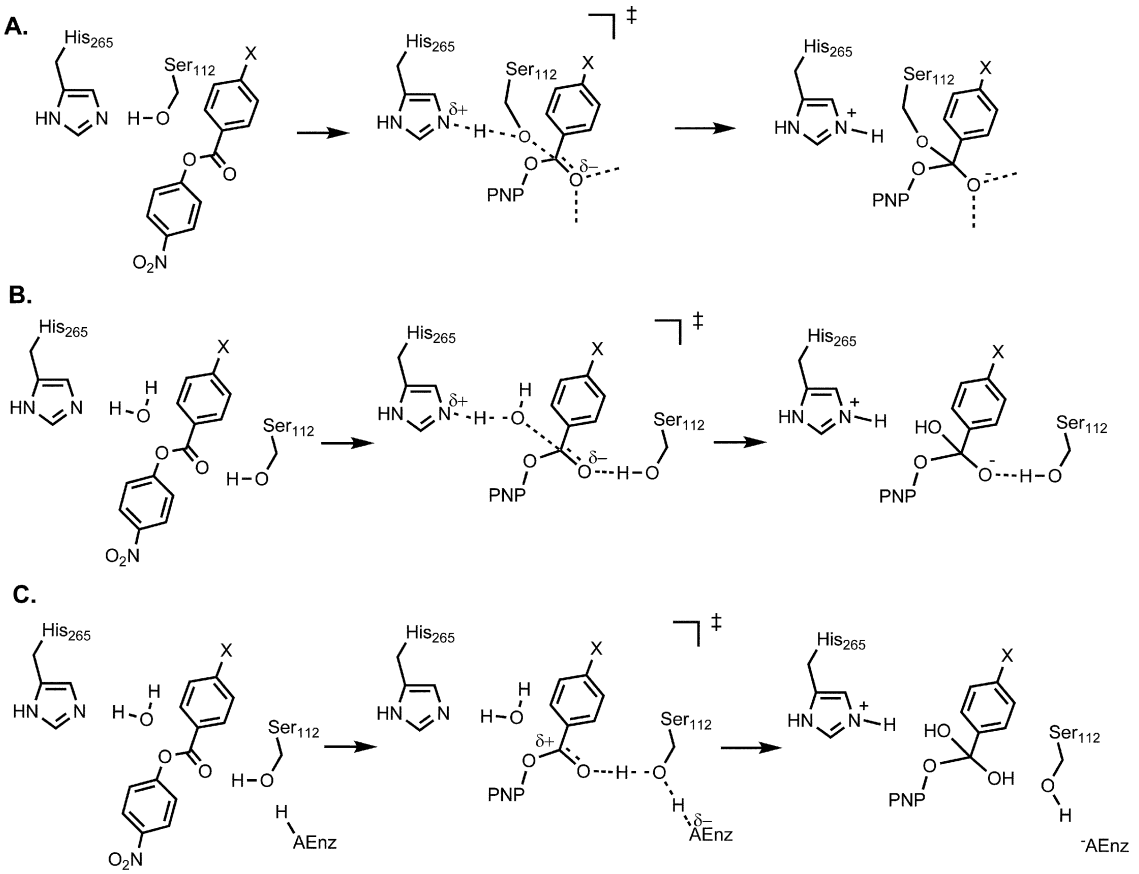

Fig. 3 Transition state structures for three possible ester hydrolysis mechanisms for BphD, involving catalytic serine as (A) a nucleophile (B) a hydrogen bond donor (C) a proton donor. Mechanism A would be completed by hydrolysis of an acyl enzyme intermediate.

Steady state kinetics

p-Nitrophenyl acetate and *p*-nitrophenyl benzoate were assayed as esterase substrates against BphD and five α/β-hydrolase enzymes: *P. fluorescens* aryl esterase,[15] *P. cepacia* lipase, *C. antarctica* lipase B, porcine pancreatic lipase, and *E. electricus* acetylcholinesterase. *P. fluorescens* aryl esterase is in the same sub-family of α/β-hydrolases as C–C hydrolases MhpC and BphD (17% sequence identity to BphD). The relative rates (in μmol min^{-1} mg protein^{-1}) are listed in Table 1. *p*-Nitrophenyl acetate is hydrolysed readily by all six enzymes, with the highest activity shown by *P. fluorescens* aryl esterase, and comparable activity for BphD and the other α/β-hydrolase enzymes. BphD showed high activity for hydrolysis of *p*-nitrophenyl benzoate, while the α/β-hydrolases showed low but detectable activity at high protein concentrations.

A series of *p*-nitrophenyl esters was assayed as substrates for BphD-catalysed ester hydrolysis. The steady-state kinetic parameters were measured, and are listed in Table 2. BphD accepts a range of aryl and alkyl esters, with the highest k_{cat} shown for *p*-nitrophenyl benzoate and *p*-nitrophenyl butyrate substrates. Determination of v_{max} over the pH range 4.0–8.5 showed one inflexion at pH 6.0 using *p*-nitrophenyl acetate as the substrate

Table 2 Steady state kinetic parameters for BphD-catalysed hydrolysis of a series of *p*-nitrophenyl esters, in 10 mM potassium phosphate buffer pH 7.0

Substrate	K_m (μM)	k_{cat} (s^{-1})	k_{cat}/K_m (M^{-1} s^{-1})
p-Nitrophenyl benzoate	1.9	4.0	2.1×10^6
p-Nitrophenyl acetate	10.0	1.3	1.0×10^5
p-Nitrophenyl propionate	9.4	2.5	3.0×10^5
p-Nitrophenyl butyrate	4.8	6.2	1.3×10^6
p-Nitrophenyl valerate	1.0	2.0	2.0×10^6
p-Nitrophenyl hexanoate	2.4	2.4	1.0×10^6

Table 1 Ester hydrolysis activity (in μmol min^{-1} mg protein^{1}) for *p*-nitrophenyl acetate (at 2 mM concentration) and *p*-nitrophenyl benzoate (at 0.1 mM concentration) by BphD and selected lipases and esterases, in 10 mM potassium phosphate buffer pH 7.0

Enzyme	*p*-nitrophenyl acetate	*p*-nitrophenyl benzoate
B. xenovorans BphD	0.14	0.69
P. fluorescens aryl esterase	20.9	8.0×10^{-4}
P. cepacia lipase	0.1	8.0×10^{-5}
C. antarctica lipase B	0.7	2.0×10^{-7}
Porcine pancreatic lipase	0.028	4.0×10^{-5}
E. electricus acetylcholinesterase	0.11	2.0×10^{-4}

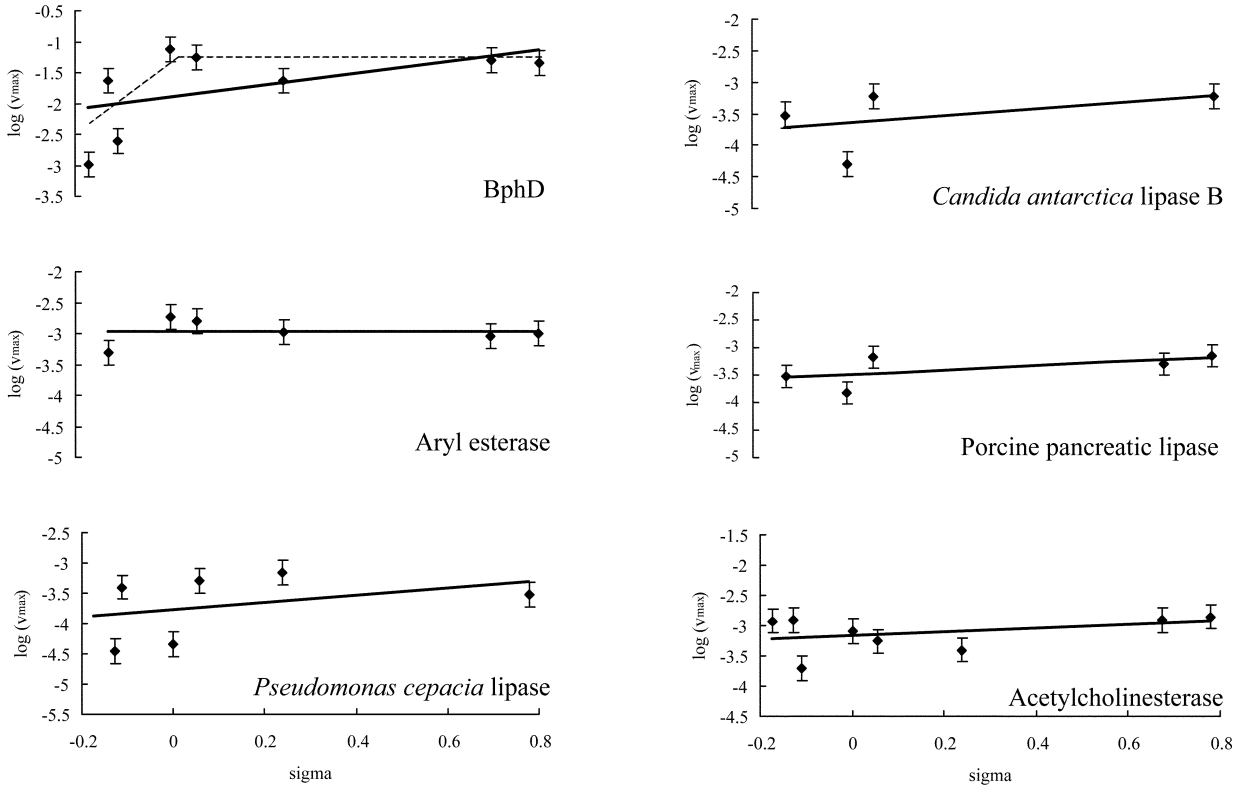

Fig. 4 Hammett plots for hydrolysis of **1–8** by BphD and lipase/esterase enzymes. Substituent coefficients (σ): NMe_2 (−0.172), Me (−0.129), MeO (−0.111), H (0.0), F (0.056), Cl (0.238), CN (0.674), NO_2 (0.778). Dashed line on BphD Hammett plot indicates alternative non-linear interpretation (see Discussion).

(data not shown), consistent with a histidine active site base, as shown previously for C–C cleavage.[12] At pH ≥ 9.0, background non-enzymatic hydrolysis was found to interfere significantly with enzyme assays.

Reaction rates were measured for BphD-catalysed hydrolysis of each of the *p*-nitrophenyl benzoates at 0.1 mM concentration ($\gg K_m$ for BphD), in 10 mM potassium phosphate buffer pH 7.0. A plot of log (v_{max}) *vs.* $\sigma$is shown in Fig. 4. The least squares gradient of this plot, corresponding to reaction coefficient ρ, is +0.98, though some non-linearity may be present (see Discussion). Kinetic analysis with the same set of substrates was carried out using *Candida antarctica* lipase B (ρ +0.56), porcine pancreatic lipase (PPL, ρ +0.40), *Pseudomonas cepacia* lipase (PCL, ρ +0.61), acetylcholinesterase from *Electrophorus electricus* (ρ +0.31), and *Pseudomonas fluorescens* aryl esterase (ρ 0.0). The results are shown in Fig. 4, and tabulated in Table 3. For some enzymes, no turnover was observed for substrates containing more bulky X = NMe_2 or OMe groups. In all but one case, a positive value of ρ was measured, in the range +0.31–0.61. In the case of *P. fluorescens* aryl esterase, there appeared to be no change in rate *vs.* σ, indicating perhaps a different rate-determining step for this enzyme.[15]

In order to examine whether the rate-limiting step in each case involved proton transfer, the solvent kinetic isotope effect upon v_{max} was measured for each enzyme, using *p*-nitrophenyl acetate as the substrate. The values are tabulated in Table 3. In each case, values in the range 1.6–2.5 were measured.

Table 3 Hammett reaction parameter ρ values for hydrolysis of *p*-substituted *p*-nitrophenyl benzoates, determined from plots shown in Fig. 4, and solvent D_2O kinetic isotope effects upon v_{max} for hydrolysis of *p*-nitrophenyl acetate

Enzyme	ρ	$v_{max}(H_2O)/v_{max}(D_2O)$
B. xenovorans LB400 BphD	0.98 ± 0.16	1.8 ± 0.04
P. fluorescens aryl esterase	0.0 ± 0.1	2.0 ± 0.01
P. cepacia lipase	0.61 ± 0.26	2.5 ± 0.03
C. antarctica lipase B	0.56 ± 0.14	2.4 ± 0.05
Porcine pancreatic lipase	0.40 ± 0.13	2.4 ± 0.03
E. electricus acetylcholinesterase	0.31 ± 0.12	1.6 ± 0.03

Pre-steady state kinetics

Pre-steady state kinetic measurements were carried out in 10 mM, pH 7.0 potassium phosphate buffer for BphD, *C. antarctica* lipase B, aryl esterase, and acetylcholinesterase, using *p*-nitrophenyl acetate as the substrate, monitoring release of *p*-nitrophenol at 410 nm. Measurements were made at 1 : 1 and 10 : 1 ratios of substrate to enzyme concentrations. For BphD, the observed data at both substrate ratios could be fitted by a single exponential, with rate constant 3.8 s^{-1} for the 1 : 1 ratio, as shown in Fig. 5A, with no observable "burst" of *p*-nitrophenol.

For the α/β-hydrolase enzymes, a "burst" of *p*-nitrophenol was observed over 0–100 ms for the reaction of *C. antarctica* lipase B with *p*-nitrophenyl acetate, as shown in Fig. 5B, and a similar burst was observed in the case of acetylcholinesterase (see Table 4). For *P. fluorescens* aryl esterase no burst was observed, and the observed

 This journal is © The Royal Society of Chemistry 2007

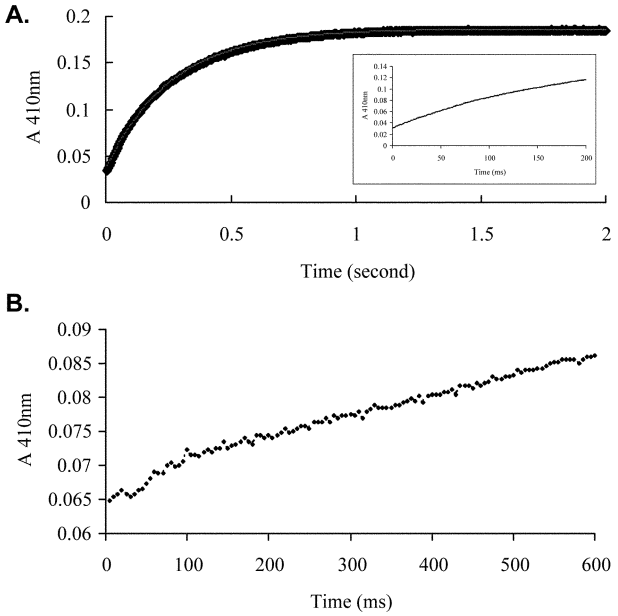

Fig. 5 Pre-steady state kinetic analysis of *p*-nitrophenyl acetate hydrolysis. (A) 1 : 1 ratio of BphD with *p*-nitrophenyl acetate; (B) 1 : 10 ratio of *C. antarctica* lipase B with *p*-nitrophenyl acetate, showing burst over 0–100 ms.

Table 4 Pre-steady state kinetic data for BphD and *P. fluorescens* aryl esterase, modelled by single exponential kinetics (A = pre-exponential factor)

Enzyme	A ($\times 10^3$)	k/s^{-1}
B. xenovorans LB400 BphD	-150.0 ± 0.2	3.8 ± 0.01
P. fluorescens aryl esterase	-118.0 ± 0.1	37.8 ± 0.1

pre-steady state data could be modelled by a single exponential. The deduced rate constants are listed in Table 4 and 5.

Kinetic analysis of S112A BphD mutant

A site-directed S112A mutant of BphD, constructed and expressed as previously described,[16] was also analysed kinetically for esterase activity. The S112A mutant showed a low but detectable level of activity for hydrolysis of *p*-nitrophenyl acetate (k_{cat} 0.0048 s^{-1}), 10^3-fold slower than wild-type BphD, and no detectable activity towards *p*-nitrophenyl benzoate. Under pre-steady state conditions, its reaction with *p*-nitrophenyl acetate could be modelled by a single exponential, with rate constant 0.011 s^{-1}, 300-fold slower than wild-type BphD.

Discussion

Three mechanisms were investigated for BphD-catalysed ester hydrolysis, involving different catalytic roles for Ser-112: A) Ser-112 as a nucleophile, as in the serine proteases; B) hydrogen bonding to oxyanion intermediate (see ref. 17 and 18 for precedent in enzyme active sites); C) protonation of oxyanion intermediate by Ser-112 (see ref. 17 and 19 for examples of serine residues acting as proton donors in enzyme-catalysed reactions).

The Hammett plot for BphD-catalysed hydrolysis of a series of *p*-nitrophenyl benzoates, shown in Fig. 4, shows an upwardly sloping plot, with a least squares gradient of +0.98, corresponding to Hammett reaction parameter ρ. This value implies a build-up of substantial negative charge in the transition state, consistent with the formation of an oxyanion intermediate. This observation rules out mechanism C, in which partial positive charge would build up upon protonation, but would be consistent with either mechanism A or B. Closer examination of the Hammett plot for BphD reveals that for substrates with $\sigma > 0$ the plot is apparently flat, while for $\sigma < 0$ the X = NMe_2 and X = OMe substrates have significantly reduced rates. These substituents are the most sterically demanding, therefore these substrates may show low turnover rates due to steric effects, or non-productive binding interactions at the enzyme active site. However, since the X = Me substrate also shows a reduced rate, an alternative interpretation is that there is a non-linear Hammett plot, with a change of rate-determining step, close to $\sigma = 0$. One observation that is consistent with this interpretation is that the pre-steady state first order rate constant for the reaction of BphD with *p*-nitrophenyl acetate (3.8 s^{-1}) is 3-fold higher than k_{cat} for this substrate (1.3 s^{-1}), indicating that product release may be rate-limiting, as found for certain site-directed mutants of C–C hydrolase MhpC.[12] Therefore, an alternative interpretation is that, for BphD-catalysed hydrolysis of substrates with $\sigma > 0$, a physical step such as product release is rate-limiting, while for substrates with electron-donating groups the rate of carbonyl addition is slowed sufficiently that it becomes rate-limiting. In this case the ρ value for $\sigma < 0$ can only be estimated to be >2. For comparison, ρ values for base-catalysed and acid-catalysed ester hydrolysis are +2.55 and −0.57, respectively.[20] Reaction of *p*-nitrophenyl benzoates with hydroxide or *p*-chlorophenoxide has been reported to give ρ values of 2.21 and 2.44 respectively.[21]

For the other α/β-hydrolase enzymes tested, positive values of ρ were found, in the range 0.31–0.61, consistent with build-up of negative charge in the transition state. Hammett analysis of a collection of lipase enzymes has been reported, using substituted phenyl butanoates,[22] in which the variable substituent is in the phenol leaving group, rather than in the acyl group as in our study. In most cases a positive ρ value was found, with the *p*-nitrophenyl

Table 5 Pre-steady state kinetic data for *C. antarctica* lipase B and *E. electricus* acetylcholinesterase, showing burst kinetics over 0–100 ms (A = pre-exponential factor)

	0–100 ms		0.1–200s	
Enzyme	A ($\times 10^3$)	k/s^{-1})	A ($\times 10^3$)	k/s^{-1})
C. antarctica lipase B	-14.5 ± 0.7	6.8 ± 0.7	-118 ± 0.1	0.029 ± 0.001
E. electricus acetylcholinesterase	-76.2 ± 8.4	7.4 ± 1.5	-1380 ± 2	0.006 ± 0.0001

substrate the highest activity for nearly all the enzymes studied,[22] which would be consistent with the positive ρ values found in this study. For serine proteases, the acylation of α-chymotrypsin by substituted phenyl acetates has been reported to give a ρ value of 1.8,[23] while a similar analysis of subtilisin gave a value of 0.87.[24]

In order to investigate the rate-determining step further, the D_2O solvent kinetic isotope effect upon V_{max} was measured in each case. Values of 1.6–2.5 were measured, consistent with the involvement of solvent water in the rate-limiting step in each case. This would be consistent either with the single step of general base mechanism B, or with the second step of nucleophilic mechanism A, namely hydrolysis of the acyl enzyme intermediate (which is known to be rate-limiting for the serine protease-catalysed hydrolysis of esters.[23])

The reactions were then studied using stopped-flow kinetics, which in the case of the serine proteases is known to exhibit burst kinetics.[25] In the case of BphD, no burst of *p*-nitrophenol was observed, and the pre-steady state data could be fitted by a single exponential, consistent with a 1-step process. These data are inconsistent with the 2-step nucleophilic mechanism A, and are consistent with the 1-step general base mechanism B for ester hydrolysis.

For the α/β-hydrolase enzymes tested, a burst of *p*-nitrophenol was observed for *C. antarctica* lipase B and acetylcholinesterase, consistent with a nucleophilic mechanism for these two enzymes. Burst kinetics have previously been observed in the hydrolysis of *p*-nitrophenyl acetate catalysed by porcine pancreatic lipase.[26] For *P. fluorescens* aryl esterase, no burst of *p*-nitrophenol was observed, indicating perhaps a fast acyl enzyme hydrolysis step.

Crystallographic studies on C–C hydrolase MhpC have shown that the catalytic Ser-110 and His-263 are both positioned above the non-cleavable analogue DKNDA. If a similar arrangement is formed during ester hydrolysis, then we propose the following mechanism, shown in Fig. 6.

Attack of water upon the ester carbonyl is catalysed by the catalytic base, His-265, to form an oxyanion intermediate, stabilised through hydrogen-bonding interactions. If the alcohol leaving group is to be protonated by His-265, then a rotation of this intermediate must occur. We propose that the catalytic serine

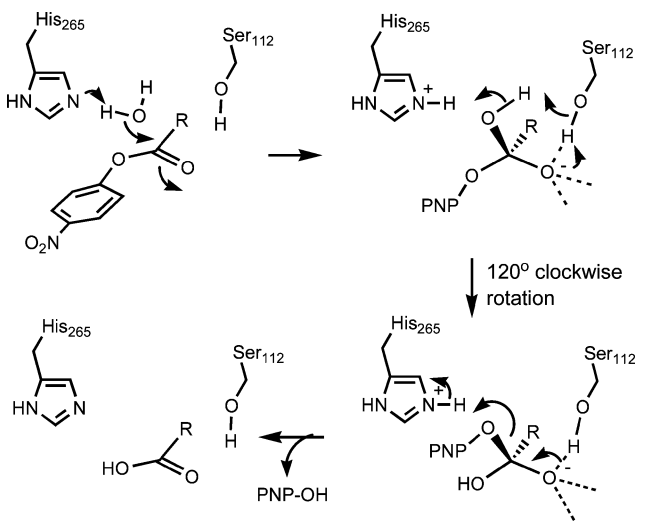

Fig. 6 Proposed mechanism for BphD-catalysed ester hydrolysis.

has two functions: it stabilises the oxyanion *via* hydrogen-bonding; and it facilitates the rotation of the oxyanion through a concerted proton transfer relay, as shown in Fig. 6. This mechanism is consistent with the kinetic results of the S112A BphD mutant, with reduced k_{cat} and one-step pre-steady state kinetics, in which these two functions are lost without Ser-112.

There are two reasons why a serine residue might be particularly well suited for these functions. Firstly, hydrogen-bonding of an alkoxide anion to an alcohol is known to be particularly strong: the strength of the hydrogen bond in the methanol–methoxide dimer in the gas phase has been estimated at 29.3 kcal mol^{-1} (122 kJ mol^{-1}).[27] In horse liver alcohol dehydrogenase, a zinc(II) alkoxide intermediate forms a very strong hydrogen bond with Ser-48 in the enzyme active site, which then mediates a proton transfer relay involving the NAD^+ 2′ hydroxyl group and His-51.[17] In addition, it has been reported that in human UDP-galactose 4-epimerase a low barrier hydrogen bond between the 4′-hydroxyl group of the sugar and O^{γ} of Ser 132 in the active site facilitates proton transfer from the sugar 4′-hydroxyl group to O^{η} of Tyr 157.[18]

Secondly, proton transfer between hydroxide ions and water is known to be a very fast and low energy process, manifested by the high ionic mobility of hydroxide ions in water.[28] The hydroxyl side-chain of serine is therefore uniquely suited to support such a mechanism.

Rotation of the oxyanion intermediate then positions a new oxygen centre in the oxyanion hole, and positions the alcohol leaving group adjacent to the protonated His-265, which functions as a proton donor. The larger value of ρ observed for BphD, relative to lipase enzymes, is consistent with increased negative charge in the transition state leading to the oxyanion intermediate.

This is a novel mechanism for ester hydrolysis by the serine catalytic triad, and is a significant departure from the generally accepted nucleophilic mechanism. As noted above, there is evidence to support the operation of a general base mechanism in the C–C cleavage reaction mechanism of MhpC and BphD. In the C–C hydrolase reaction, there is no apparent need for rotation of the oxyanion intermediate, but the active site serine would provide stabilisation of the gem-diolate intermediate through hydrogen-bonding. From kinetic analysis of a S110A mutant of MhpC, it has been calculated that the hydroxyl group of Ser-110 provides 23 kJ mol^{-1} transition state stabilisation for C–C cleavage, which could be accounted for by a strong hydrogen bond. More widely, in the α/β-hydrolase family, it has been proposed that a general base mechanism occurs in hydroxynitrile lyase from *Hevea brasiliensis*,[19] therefore it seems possible that general base mechanisms might occur more widely in this family of enzymes, and might help to rationalise the range of diverse activities observed.[3]

Experimental

Materials

Wild-type *Burkholderia xenovorans* LB400 BphD and the S112A BphD mutant were overexpressed and purified as previously described.[16] *Pseudomonas fluorescens* aryl esterase was expressed as a C-terminal His_6 fusion protein from plasmid pJOE2792, as previously reported.[29] *Pseudomonas cepacia* lipase, *Candida antarctica* lipase B, porcine pancreatic lipase and *Electrophorus*

 This journal is © The Royal Society of Chemistry 2007

electricus acetylcholinesterase were purchased from Fluka Biochimika. All other chemicals and biochemicals were purchased from Sigma-Aldrich.

Synthesis of *p*-nitrophenyl *p*-substituted benzoate substrates

Substrates **1–8** were synthesized using literature procedures,[13,14] either from the *p*-substituted benzoic acid and *p*-nitrophenyl chloroformate (**1–6**), or from the *p*-substituted benzoyl chloride and *p*-nitrophenol (**7**, **8**). NMR and MS data were identical with literature data (ref. 13 and 14).

Steady-state kinetic measurements

Esterase activity of BphD against *p*-nitrophenyl esters (data in Table 2) was assayed in 1.0 ml of 10 mM potassium phosphate buffer pH 7.0 at 25 °C on a Cary 1 UV–vis spectrophotometer by monitoring the appearance of *p*-nitrophenol at 410 nm. K_m and k_{cat} values were determined using Lineweaver–Burk plots. All other enzyme assays were carried out in 200 µl of 10 mM potassium phosphate buffer pH 7.0 at 25 °C on a Genios fluorometer (Tecan), monitoring the appearance of *p*-nitrophenol at 400 nm over 30 min. The assays were done in duplicate. Substrates were dissolved in an appropriate amount of DMSO. For Hammett plot studies, *p*-substituted *p*-nitrophenyl benzoate esters were assayed at a final concentration of 100 µM. For solvent kinetic isotope effect determination, *p*-nitrophenyl acetate (final concentration 2 mM) was used as a substrate, using 99% deuterium oxide as the solvent, in deuterated buffer.

Pre-steady state kinetics measurements

The pre-steady state kinetic assays for BphD, *C. antarctica* lipase B, aryl esterase, and acetylcholinesterase were carried out on a DX.17MV stopped-flow spectrometer (Applied Photophysics Ltd) using *p*-nitrophenyl acetate as the substrate. The enzymes and substrate were dissolved in 10 mM potassium phosphate buffer, pH 7.0. In each single stopped-flow experiment, solutions of 1.0 mg ml^{-1} enzyme (14–32 µM) and substrate were mixed in a 1 : 1 or 1 : 10 [E] : [S] ratio, at 25 °C. The appearance of *p*-nitrophenol was monitored at 410 nm. Data for every single shot were simulated with single, double or treble-exponential kinetics models, and the best-fit rate constants and amplitudes were calculated.

Acknowledgements

This work was supported by BBSRC (research grant B20467). We are grateful to Professor R. J. Kazlauskas (University of Minnesota) for the provision of the *P. fluorescens* aryl esterase expression plasmid.

References

1 D. L. Ollis, E. Cheah, M. Cygler, B. Dijkstra, F. Frolow, S. M. Franken, M. Harel, S. J. Remington, I. Silman, J. Schrag, J. L. Sussman, K. H. G. Verschueren and A. Goldman, *Protein Eng.*, 1992, **5**, 197–211.
2 J. D. Schrag and M. Cygler, *Methods Enzymol.*, 1997, **284**, 85–107.
3 T. D. H. Bugg, *Bioorg. Chem.*, 2004, **32**, 367–375.
4 W. W. Y. Lam and T. D. H. Bugg, *Biochemistry*, 1997, **36**, 12242–12251.
5 S. Y. K. Seah, G. Terracina, J. T. Bolin, P. Riebel, V. Sniekus and L. D. Eltis, *J. Biol. Chem.*, 1998, **273**, 22943–22949.
6 E. Diaz and K. N. Timmis, *J. Biol. Chem.*, 1995, **270**, 6403–6411.
7 I. M. J. Henderson and T. D. H. Bugg, *Biochemistry*, 1997, **36**, 12252–12258.
8 J.-J. Li and T. D. H. Bugg, *Chem. Commun.*, 2005, 130–132.
9 S. M. Fleming, T. A. Robertson, G. J. Langley and T. D. H. Bugg, *Biochemistry*, 2000, **39**, 1522–1531.
10 D. M. Speare, S. M. Fleming, M. N. Beckett, J.-J. Li and T. D. H. Bugg, *Org. Biomol. Chem.*, 2004, **2**, 2942–2950.
11 G. Dunn, M. G. Montgomery, F. Mohammed, A. Coker, J. B. Cooper, T. A. Robertson, J.-L. Garcia, T. D. H. Bugg and S. P. Wood, *J. Mol. Biol.*, 2005, **346**, 253–265.
12 C. Li, M. G. Montgomery, F. Mohammed, J.-J. Li, S. P. Wood and T. D. H. Bugg, *J. Mol. Biol.*, 2005, **346**, 241–251.
13 S. Kim, J. I. Lee and Y. C. Kim, *J. Org. Chem.*, 1985, **50**, 560–565.
14 C. D. Erba, F. Sancassan, G. Leandri, M. Novi, G. Petrillo and A. Mele, *Gazz. Chim. Ital.*, 1989, **119**, 643–647.
15 P. Bernhardt, K. Hult and R. J. Kazlauskas, *Angew. Chem., Int. Ed.*, 2005, **44**, 2742–2746.
16 J.-J. Li, C. Li, C. A. Blindauer and T. D. H. Bugg, *Biochemistry*, 2006, **45**, 12461–12469.
17 P. K. Agarwal, S. P. Webb and S. Hammes-Schiffer, *J. Am. Chem. Soc.*, 2000, **122**, 4803–4812.
18 J. B. Thoden, T. M. Wohlers, J. L. Fridovich-Keil and H. M. Holden, *Biochemistry*, 2000, **39**, 5691–5701.
19 J. Zuegg, K. Gruber, M. Gugganig, U. G. Wagner and C. Kratky, *Protein Sci.*, 1999, **8**, 1990–2000.
20 N. S. Isaacs, *Physical Organic Chemistry*, Longman Press, Harlow, 1987, pp. 131–146.
21 I.-H. Um, E.-K. Chung and D.-S. Kwon, *Tetrahedron Lett.*, 1997, **38**, 4787–4790.
22 U. T. Bornschauer, G. Rodriguez Ordonez, A. Hidalgo, A. Gollin, J. Lyon, T. S. Hitchman and D. P. Weiner, *J. Mol. Catal. B: Enzym.*, 2005, **36**, 8–13.
23 M. L. Bender and K. Nakamura, *J. Am. Chem. Soc.*, 1962, **84**, 2577–2582.
24 L. T. Kanerva and A. M. Klibanov, *J. Am. Chem. Soc.*, 1989, **111**, 6864–6865.
25 H. Gutfreund and J. M. Sturtevant, *Biochem. J.*, 1956, **63**, 656–661.
26 C. Chapus, M. Sémériva, C. Bovier-Lapierre and P. Desnuelle, *Biochemistry*, 1976, **15**, 4980–4987.
27 G. J. C. Paul and P. Kebarle, *J. Phys. Chem.*, 1990, **94**, 5184–5189.
28 R. Chang, *Physical Chemistry for the Chemical and Biological Sciences*, University Science Books, Sausalito, California, 2000, p. 254.
29 J. D. Cheeseman, A. Tocilj, S. Park, J. D. Schrag and R. J. Kazlauskas, *Acta Crystallogr., Sect. D: Biol. Crystallogr.*, 2004, **D60**, 1237–1243.